



ELSEVIER

Journal of Alloys and Compounds 315 (2001) 51–58

Journal of  
ALLOYS  
AND COMPOUNDS

www.elsevier.com/locate/jallcom

# Improved equations for addressing the high pressure melting of metastable silicate perovskites

Zhongwu Wang<sup>a,\*</sup>, Bertram Schott<sup>b</sup>, Peter Lazor<sup>b</sup>, S.K. Saxena<sup>a</sup><sup>a</sup>Center for Study of Matter at Extreme Conditions (CeSMEC), Department of Earth Sciences, Florida International University, University Park, Miami, FL 33199, USA<sup>b</sup>Institute of Earth Sciences, Uppsala University, S-752 36 Uppsala, Sweden

Received 4 September 2000; accepted 16 October 2000

## Abstract

Based on our previous thermodynamic model of high pressure melting of any solid that is stable under ambient pressure (Wang et al., *J. Alloys Comp.* 299 (2000) 287–291), we have derived a few equations to calculate the melting temperatures of the metastable phases synthesized at high pressures. Compared to obtained results of high pressure melting of pyrope ( $\text{Mg}_3\text{Al}_2\text{Si}_3\text{O}_{12}$ ) stable at ambient condition, both  $\text{CaSiO}_3$  and  $\text{MgSiO}_3$  perovskites have been used to calculate the melting temperatures at high pressures. The reliability of the improved model has been well demonstrated by a reasonable agreement between the calculated melting temperatures and experimental data. Comparison between obtained results with those estimated by the empirical melting equations indicates that our model is more precise than the empirical melting equations in extrapolating the melting temperatures at higher pressures. © 2001 Elsevier Science B.V. All rights reserved.

**Keywords:** Ceramics; Equation of state; High pressure; Phase transitions

## 1. Introduction

The melting behavior of any solid under extreme conditions has attracted the attention of theoretical [2] and experimental workers [3]. The approaches to solve the problems involved are based on the newly developed in-situ laser heating DAC techniques [4], first-principle theoretical simulations [2] and empirical melting law predictions [5,6]. Due to the fact that it is time-consuming and requires a strong theoretical physics background, ab-initio theoretical simulation is hard as a popular tool to predict the melting of solids at high pressures. The in-situ laser heating DAC technique allows one to discover the melting at pressures up to 100 GPa [7], but the need of pressure medium along with high melting points greatly limits our experimental investigation on the melting mechanism of refractory materials at high pressure, such as silicates. So far, the estimates of melting of solids at high pressures have depended upon a few empirical melting equations, including Lindemann, Simon and Kraut-Kennedy equations [8–10]. As is well known, those equations

are only validated by comparison between estimated melting temperatures and experimental data at lower pressures ( $<7$  GPa), which can be reached by traditional high-pressure techniques, such as piston-cylinder apparatus. Therefore, new high-pressure Diamond Anvil Cell (DAC) laser heating data indicate that the estimates by the empirical melting equations significantly deviate from the actual melting, showing a higher slope of  $dT_m/dP$  [11].

In this case, we employed the thermal parameters of solids experimentally determined at ambient conditions, and developed a reliable thermodynamic model [1], which can well extrapolate the melting temperatures of solids under extreme compression. Unfortunately, the model only works well for solids that are stable at ambient conditions, but the model is not valid to estimate the melting temperatures of high-pressure metastable phases, which only occur or remain stable at in-situ high-pressure conditions. To better address this issue, combining the lattice dynamics [12] with our thermodynamic model [1], improved equations have been derived to extrapolate the melting temperatures of high-pressure phase of solids.

As the most important industrial materials, different refractory silicates including high-pressure phases have been synthesized. High-pressure mineral physics studies

\*Corresponding author. Fax: +1-305-348-3070.

E-mail address: zwang04@fiu.edu (Z. Wang).

indicate that both  $\text{CaSiO}_3$  and  $\text{MgSiO}_3$  perovskites are only synthesized at high-pressure conditions [13,14], which have higher bulk modulus and higher melting temperatures. Meanwhile, both  $\text{CaSiO}_3$  and  $\text{MgSiO}_3$  perovskites are the most important and most abundant constituents of the Earth's interior. The melting temperatures of both of these minerals at high pressures may have important implications for the chemistry and physics of the Earth's interior [13,14]. So far, the  $P$ - $V$ - $T$  equations and the melting data of both perovskites have been generated up to 70 GPa by different high-pressure techniques [3,14,15]. The thermal parameters at the perovskite-forming pressure can be obtained by our newly derived equations, and thus the existing experimental melting data allow us to compare the obtained results, and to test the reliability of the improved model. In this paper, pyrope ( $\text{Mg}_3\text{Al}_2\text{Si}_3\text{O}_{12}$ ) is first used to describe the old model. Then, both  $\text{CaSiO}_3$  and  $\text{MgSiO}_3$  perovskites are employed to clarify the newly improved model. Finally, the empirical melting equation is used to duplicate the melting curves of the above silicates, and a comparison between calculated melting curves and experimental data is used to explore the reliability and advantages of the model.

## 2. Method of analysis

The method for calculating the stable phase at ambient conditions is the same as that employed by Wang et al. [1] in estimating the melting of  $\text{Al}_2\text{O}_3$  at high-pressures. The theory is based on the relation of thermal expansion and temperature [16,17]. Assuming the melting at any pressure has similar microscopic thermodynamic characteristics, the thermal parameters experimentally determined at ambient condition are used to extrapolate the melting of solids at high-pressure. Firstly, we start at  $T=300$  K as the reference state, and then define the critical state at melting temperature. When a solid reaches the critical state, an infinite input of energy provided by heating melts the solid. Therefore, the observed melting temperature represents the lower limit of melting temperatures of solids. At any given pressure, the volumes both at the reference state ( $T=300$  K) and at the critical state ( $T$ =melting temperature) are defined as the reference volume ( $V_0$ ) and the critical volume ( $V_C$ ), respectively.

Based on the thermodynamic relation between isobaric thermal expansion  $\alpha_p$  and isothermal compressibility  $\beta_T$  [16–18]:

$$\left(\frac{\partial \alpha_p}{\partial P}\right)_T = -\left(\frac{\partial \beta_T}{\partial T}\right)_P \quad (1)$$

we note that the locus of temperature extrema of  $\beta_T$  along isobars coincides with the locus of pressure extrema of  $\alpha_p$  along isotherms. This clearly indicates that the  $\beta_T$  is closely correlated to thermal expansion. Combining with the isothermal bulk modulus  $K_T$  and the  $\beta_T$  with the

relation of  $K_T = 1/\beta_T$ , it is valid to allow to exchange  $K_T$  at two temperatures to obtain an average approximation, and then run our calculation at high-pressure. Thus, the critical volumes ( $V_C$ ) corresponding to the critical temperatures can be obtained with the Birch–Murnaghan equation [16] using the isothermal bulk modulus at 300 K ( $K_0$ ) at high pressures based on the above thermodynamic analysis. The reference volume ( $V_0$ ) at ambient condition can be calculated from the isothermal bulk modulus at the critical temperature ( $K_T$ ).

With the above method, the critical volume ( $V_C$ ) and the reference volume ( $V_0$ ) at different pressures can be obtained. The difference between the two volumes at one given pressure can be assumed as the thermal expansion caused by increasing temperature from the reference temperature to the critical temperature. The pressure corresponding to this thermal expansion is the thermal pressure ( $\Delta P_{\text{th}}$ ), which can be obtained using the following equation [16]:

$$\Delta P_{\text{th}} = \frac{3}{2} K_C [(V_{C,P}/V_{0,P})^{(7/3)} - (V_{C,P}/V_{0,P})^{(5/3)}] \cdot \left\{ 1 + \frac{3}{4} (K' - 4) [(V_{C,P}/V_{0,P})^{(2/3)} - 1] \right\} \quad (2)$$

where  $V_{0,P}$  and  $V_{C,P}$  are the volumes at 300 K and at the critical temperature under different pressures, respectively.  $K'$  is the bulk modulus derivative, and  $K_C$  is the isothermal bulk modulus at the critical temperature. Because the above process can be assumed to be the compression from the critical to the reference state, it is reasonable to employ  $K_C$  in calculating the thermal pressure.

At any temperature ( $T$ ) and for a given volume ( $V$ ) of a solid, the pressure ( $P$ ) can be expressed at the sum of the static pressure at a reference temperature ( $T_0$ ) and the thermal pressure ( $\Delta P_{\text{th}}$ ),

$$P(V,T) = P(V,T_0) + \Delta P_{\text{th}} \quad (3)$$

If  $T_0$  is taken as the room temperature ( $T_0 = 300$  K) then,

$$\Delta P_{\text{th}} = P(T) - P(300 \text{ K}) \quad (4)$$

Based on the studies of Anderson [16,17], assuming that the  $\alpha K_T$  is constant and that thermal pressure is independent of volume, we could calculate the thermal pressure  $\Delta P_{\text{th}}$  with:

$$\Delta P_{\text{th}} = P_{\text{th}} - P_{\text{th}}(300) = \bar{\alpha} \bar{K}_T (T - T_0(300 \text{ K})) \quad (5)$$

Combining Eqs. (2) and (5), the melting temperature at different pressures can be calculated by [1,18]

$$T_m = \frac{\Delta P_{\text{th}}}{\bar{\alpha} \bar{K}_T} + T_0(300 \text{ K}) \quad (6)$$

For calculating the melting of high-pressure phases which are not quenchable at ambient conditions, the

thermal parameters should be first obtained. To this end, the crystal lattice dynamics is employed to derive a few equations, which allow us to calculate the corresponding thermal parameters at a high pressure phase-forming pressure. The pressure  $P(V, T_0)$  can be expressed in terms of the volume derivative of the potential energy  $U$  of the lattice as [12,19]

$$P(V, T) = -dU/dV + \Delta P_{th}. \quad (7)$$

The potential energy  $U$  can be expressed in a Taylor series in powers of the volume change  $X = V - V_0$  [12,19]:

$$U = U_0 + U'_0 X + U''_0 \frac{X^2}{2} + U'''_0 \frac{X^3}{6} \quad (8)$$

where  $U'_0$ ,  $U''_0$  and  $U'''_0$  are the first-, second- and third-order volume derivatives of  $U$  with respect to  $V$  taken at  $V = V_0$ . Equilibrium conditions like isothermal conditions yield  $U'_0 = 0$ . Values of  $U''_0$  and  $U'''_0$  are determined using the expressions for isothermal bulk modulus  $K_T$  and its pressure derivatives given by

$$K_T = -V \left( \frac{dP}{dV} \right)_T = V \left( \frac{d^2 U}{dV^2} \right)_T \quad (9)$$

and

$$\begin{aligned} \frac{dK_T}{dP} &= -1 - V \frac{\left( \frac{d^2 P}{dV^2} \right)_T}{\left( \frac{dP}{dV} \right)_T} \\ &= -1 - V \frac{\left( \frac{d^3 U}{dV^3} \right)_T}{\left( \frac{d^2 U}{dV^2} \right)_T} \end{aligned} \quad (10)$$

The condition  $V = V_0$  at  $P = 0$  reduces Eqs. (9) and (10) to  $U''_0 = K_0/V_0$  and  $U'''_0 = -[K_0(K'_0 + 1)]/V_0^2$ , where  $K_0$  and  $K'_0$  are the values of  $K_T$  and  $dK_T/dP$  at  $P = 0$  and  $T = 300$  K, respectively. Now,  $dU/dV$  can be calculated from Eq. (8) and substituted into Eq. (7) resulting in a quadratic equation in  $X/V_0$  which can be solved yielding [19,20]

$$\begin{aligned} \frac{X}{V_0} &= \frac{V}{V_0} - 1 \\ &= \frac{1 - [1 - (2(K'_0 + 1)/K_0)(\Delta P_{th} - P)]^{1/2}}{(K'_0 + 1)}. \end{aligned} \quad (11)$$

The above formula can be used to estimate the volume ( $V$ ) of a solid under simultaneously high temperature and high pressure conditions, and it can also be used to calculate the critical volume corresponding to the melting temperature at reference pressure [1,11]. The reference pressure is the pressure at which the high-pressure phase is formed.

Employing the relation of  $K_T$  and temperature, we can obtain the  $K_T$  value at melting temperature and at reference pressure. Then, combining the thermodynamic analysis [1,11] and employing the third-order Birch–Murnaghan equation of state (EOS) [16], we can calculate the reference volume at 300 K at reference pressure for the high-pressure phase of any solid.

As all the thermal parameters have been obtained for high-pressure phase at reference pressure (the high pressure phase-forming pressure), the reference volumes ( $T_0 = 300$  K) and the critical volumes corresponding to the melting point under high pressures can be obtained [1,11]. Then, using the same method mentioned above in calculating the melting temperatures of solids being stable at ambient condition, the melting temperatures of high-pressure (metastable) phases at high pressure can be obtained.

### 3. Results and discussion

#### 3.1. Pyrope ( $Mg_3Al_2Si_3O_{12}$ )

Pyrope is of cubic structure, and is stable at ambient condition. Based on the available thermal parameters (Table 1), the reference volume and the critical volumes at high pressure are obtained as shown in Fig. 1 and Table 2. The thermal pressures corresponding to the thermal expansion from reference state to critical state are shown in Fig. 2 and Table 2, and the calculated melting temperatures of

Table 1  
Thermal parameters used in our fits<sup>a</sup>

Minerals	$K_{300}$ (GPa)	$K_C$ (GPa)	$V_{300}$ (Å <sup>3</sup> /unit cell)	$V_C$ (Å <sup>3</sup> /unit cell)	$\bar{\alpha} \bar{K}_T$ (average) (10 <sup>-3</sup> )	$K'$
$Mg_3Al_2Si_3O_{12}$	172.8	128.8	113.3	119.5	4.45	4.0
$CaSiO_3$	232	137.62	41.59	46.07	7.20	4.8
$MgSiO_3$	261	176.44	142.52	155.57	6.92	4.0

<sup>a</sup> The thermal parameters for pyrope ( $Mg_3Al_2Si_3O_{12}$ ) are from Anderson et al. [17] and volume is cm<sup>3</sup>/mol. The thermal parameters for  $CaSiO_3$  perovskite are based on Wang et al. [15], and that for  $MgSiO_3$  perovskite are from Funamori et al. [14]. Here we choose the reference pressure for  $CaSiO_3$  with 16 GPa, and for  $MgSiO_3$  with 26 GPa, which are somewhat higher than the perovskite-forming pressure, and this makes sure that both minerals are exactly of perovskite structure. At the corresponding reference pressures, the melting temperatures of  $CaSiO_3$  and  $MgSiO_3$  perovskites are 2860(±70) K (16 GPa) and 3020(±100) K (26 GPa), respectively (Shen and Lazor [3]).

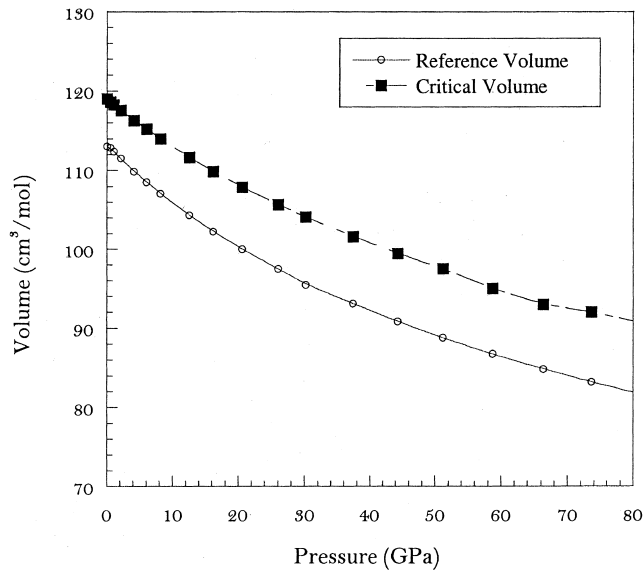


Fig. 1. The critical and reference volumes for pyrope ( $\text{Mg}_3\text{Al}_2\text{Si}_3\text{O}_{12}$ ) under high pressures.

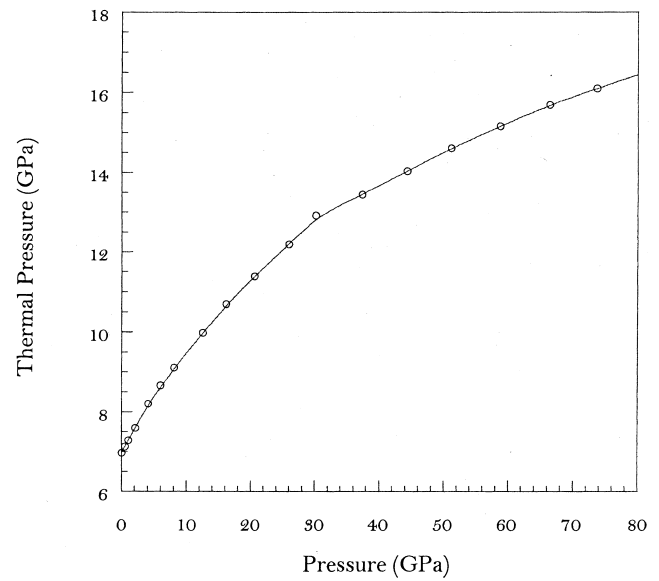


Fig. 2. The thermal pressures of pyrope ( $\text{Mg}_3\text{Al}_2\text{Si}_3\text{O}_{12}$ ) under high pressures.

pyrope are shown in Table 2 and in Fig. 3, along with available experimental data [3,21–23].

To judge the melting of pyrope directly from garnet structure phase at high pressure, it is important to clarify the phase diagram of pyrope at high temperature and high pressures. For the phase transformation of pyrope at high temperature high-pressure condition, so far, there exists a great disagreement for existing experimental data [24–29] (Fig. 4). First, Liu [24] observed a phase transformation from garnet to the ilmenite structure at  $\sim 24$  GPa and then to the perovskite structure at  $\sim 30$  GPa and at about  $1000^\circ\text{C}$  using a YAG laser heating diamond anvil cell. The phase transformation from pyrope (garnet structure) to ilmenite

structure was also confirmed by Kanzaki [25], by means of a multi-anvil device using the glass with the same composition of pyrope as a starting material. Later, Irifune et al. [26] used a multi-anvil device, and found that pyrope transforms to an aluminous perovskite plus a corundum ( $\text{Al}_2\text{O}_3$ )/ilmenite ( $\text{MgSiO}_3$ ) solid solution at 26.5 GPa and at  $1500^\circ\text{C}$ . Meanwhile, Kesson et al. [27] found that pyrope garnet completely incorporates into a perovskite structure at  $\sim 60$  GPa with same composition. In contrast, Ahmed-zaid and Madon [28] observed a newly additional aluminous phase at  $\sim 45$  GPa. Combining the previous results, Serghiou et al. [29] employed a laser-heating

Table 2

The calculated results of pyrope ( $\text{Mg}_3\text{Al}_2\text{Si}_3\text{O}_{12}$ )

Pressure (GPa)	Reference volume ( $\text{cm}^3/\text{mol}$ )	Critical volume ( $\text{cm}^3/\text{mol}$ )	Thermal pressure (GPa)	Melting temperature (K)
0	113.31	119.50	6.975	1867
0.521	112.85	118.64	7.130	1884
1.046	112.42	118.29	7.286	1850
2.111	111.52	117.59	7.595	1916
4.112	109.89	116.32	8.208	2047
5.987	108.52	115.2	8.661	2143
8.111	107.09	113.98	9.107	2238
12.551	104.33	111.63	9.980	2424
16.162	102.26	109.88	10.695	2576
20.612	100.11	107.89	11.383	2722
26.001	97.504	105.68	12.191	2894
30.184	95.451	104.11	13.311	3132
37.422	93.098	101.62	13.448	3161
44.266	90.858	99.498	14.034	3286
51.181	88.793	97.541	14.607	3408
58.746	86.753	95.582	15.156	3525
66.361	84.869	93.775	15.694	3640
73.651	83.248	92.177	16.092	3724
80.883	81.746	90.701	16.487	3808

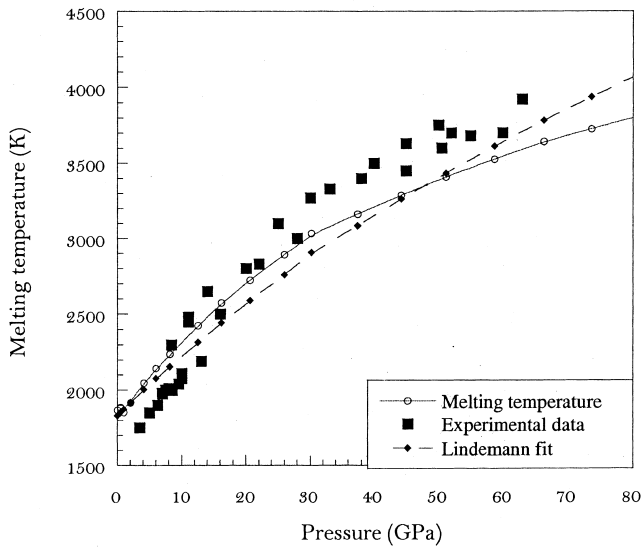


Fig. 3. The melting temperatures of pyrope ( $\text{Mg}_3\text{Al}_2\text{Si}_3\text{O}_{12}$ ) under high pressures.

diamond cell, which has small pressure and temperature gradients across the loading sample section at very high  $P$ - $T$  conditions, re-evaluated the phase diagram of pyrope, and concluded that pyrope first transforms to an ilmenite structure at 21.5 GPa; to perovskite plus ilmenite phase at above 24 GPa; to perovskite plus a small amount of  $\text{Al}_2\text{O}_3$  above 29 GPa; and to pure perovskite phase at pressure above 43 GPa. This leads us to assume that pyrope remains stable in the garnet structure at least up to 22 GPa and at temperature lower than the melting point. In a comparison with our calculated melting curve, it is shown that our result is in reasonable agreement with the experimental data [3,21–23], which correspond to the pressure range for the melting of pyrope directly from garnet structure. It is pointed out that the employed thermal parameter data are from garnet-structure pyrope, so it is reasonable that the

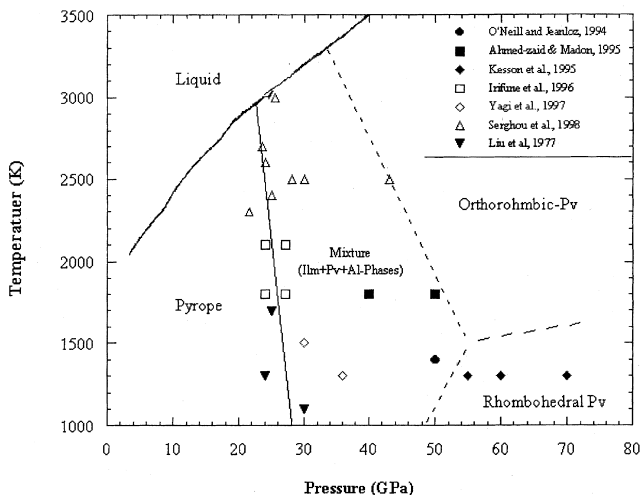


Fig. 4. The phase diagram of pyrope ( $\text{Mg}_3\text{Al}_2\text{Si}_3\text{O}_{12}$ ) at high temperatures and high pressures.

obtained results only agree with the melting of pyrope at the pressure stability range of garnet phase. Thus, it is easily concluded that our model can well reproduce the melting of pyrope up to the phase transformation pressure of garnet structure phase.

As for a comparison, the melting estimates using Lindemann melting equation are also given. As is well known, it is valid for the Lindemann equation to evaluate the high pressure melting of simple compounds [8,9], but this is only supported by a comparison to the experimental data at quite lower pressures, which is the pressure range reached by the traditional high pressure techniques [10,23]. Without more powerful empirical means, those equations are also used to extrapolate the high pressure melting of other solids at higher pressure [4]. Thus, this raises questions on the reliability of the Lindemann melting equation to estimate the melting of solids under extreme compression.

For the Lindemann melting law, the Slater Gruneisen parameter ( $\gamma$ ), as an important input parameter, can be estimated to be 1.83, based on the relation  $\gamma = 1/2(K' - 1/3)$ , and  $K'$  is the isothermal bulk modulus derivative [5,6]. Thus, assuming that  $\rho_0\gamma_0 = \rho\gamma$ , the fitted curves can be obtained using the following formula:

$$T_m = T_{m0} \text{Exp}(2\gamma_0(1 - \rho_0/\rho) + 2/3 \ln(\rho_0/\rho)) \quad (12)$$

where  $T_m$  and  $T_{m0}$  are the melting temperatures at high pressure and at 1 atm, respectively;  $\rho_0$  and  $\rho$  are the densities at one atmosphere pressure and at high pressures, respectively.

It has been well shown in Fig. 3 that the Lindemann equation cannot give a precise estimate for the melting for pyrope, due to a higher melting slope ( $dT_m/dP$ ), which significantly deviates from the actual melting at higher pressures [3,21–23]. As a reliable and practical method, our calculated curve indicates that our model can well reproduce the melting of pyrope from lower and high pressure.

### 3.2. $\text{CaSiO}_3$ perovskite

$\text{CaSiO}_3$  perovskite can be synthesized at pressures above 13.5 GPa, and it remains stable at least up to 135 GPa [30], but upon the release of pressure to ambient conditions, it transforms to an amorphous phase [13]. It is clearly shown that  $\text{CaSiO}_3$  perovskite cannot be obtained at ambient condition, so it is not possible to calculate the melting temperatures at high pressure only based on our previous model [1] which was applied to calculate the melting of pyrope and  $\text{Al}_2\text{O}_3$ . Fortunately, the improved equations combined with our old model allow us to calculate the melting of  $\text{CaSiO}_3$  perovskite at high pressures.

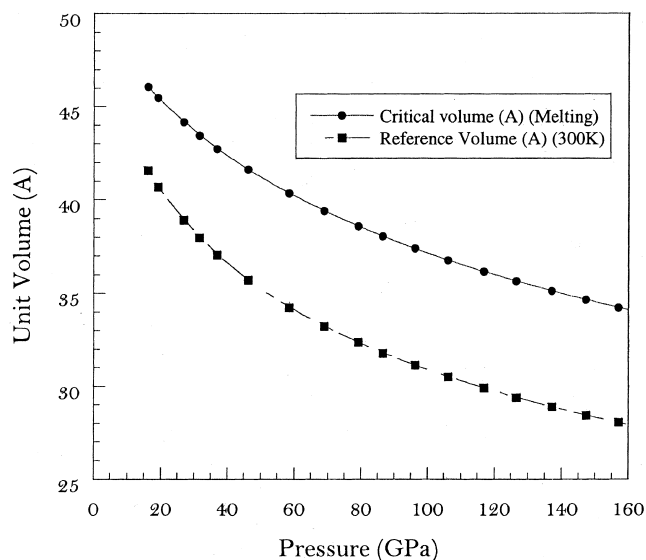
The available thermal parameters are based on Wang et al. [15], as shown in Table 1. The reference pressure is

Table 3

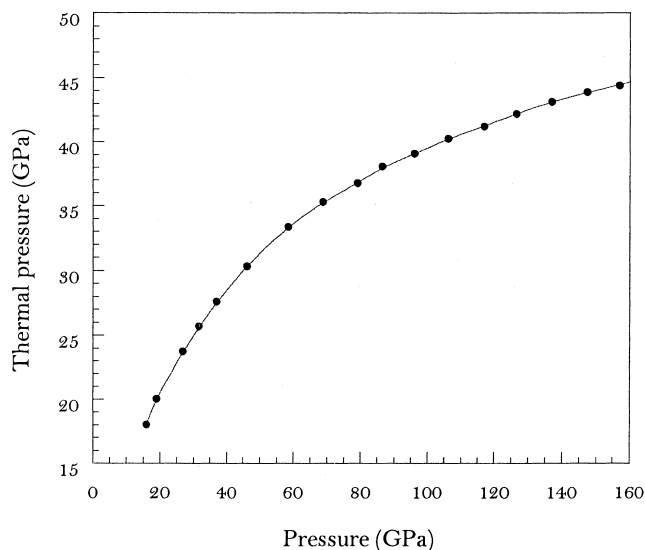
The calculated results of  $\text{CaSiO}_3$  perovskite

Pressure (GPa)	Reference volumes ( $\text{\AA}/\text{unit cell}$ )	Critical volumes ( $\text{\AA}/\text{unit cell}$ )	Thermal pressure (GPa)	Melting temperature (K)
16.00	46.07	41.59	18.04	2806
19.09	45.48	40.69	20.02	3081
26.81	44.17	38.91	23.75	3598
31.55	43.47	37.98	25.70	3869
36.88	42.74	37.07	27.63	4137
46.12	41.62	35.73	30.35	4515
58.41	40.34	34.26	33.40	4939
68.79	39.41	33.24	35.32	5206
79.10	38.59	32.39	36.77	5406
86.51	38.05	31.80	38.09	5590
96.11	37.40	31.15	39.08	5728
106.23	36.77	30.51	40.28	5895
116.88	36.16	29.92	41.23	6026
126.44	35.66	29.41	42.21	6163
136.96	35.14	28.91	43.16	6294
147.35	34.67	28.45	43.89	6395
156.93	34.26	28.06	44.42	6469
165.59	33.90	27.71	45.21	6579

$P_0 = 16$  GPa, which is a little higher than the perovskite forming pressure of 13.5 GPa [13,30]. Table 3 shows the results we got, when substituting the given thermal parameters into series of our model formula. Under high pressures, the reference and the critical volumes show a reasonable decrease, which is consistent with the high-pressure behaviors, such as the high-pressure compressibility of solids (Fig. 5). The given thermal pressures at different pressures contribute to the pressure values, which are due to a heating-induced expansion of solid from reference state to critical state (Fig. 6). The calculated melting temperatures are in agreement with the experimental data given by Shen and Lazor [3] and Zerr et al. [31], respectively (Fig. 7).

Fig. 5. The reference volumes and critical volumes of  $\text{CaSiO}_3$  perovskite at high pressures.

Compatibility between our calculated results and the recent experimental data by Zerr et al. [31] is reasonably high, whereas there is a significant difference between our results and the experimental results of Shen and Lazor [3]. This is because the laser heating DAC technique may cause a measuring error in temperature determination due to a chemical reaction occurring between the pressure medium and the sample [31,32]. Thus, in comparison with the employed medium using the same laser heating technique in experiments, carried out by two different groups, Shen and Lazor's [3] data may underestimate the melting temperatures of  $\text{CaSiO}_3$  perovskite. Zerr et al. [31] took into account the influence of a chemical reaction between the pressure medium and the sample, yielding more exact high pressure melting temperatures of  $\text{CaSiO}_3$ .

Fig. 6. The thermal pressures of  $\text{CaSiO}_3$  perovskite under high pressures.

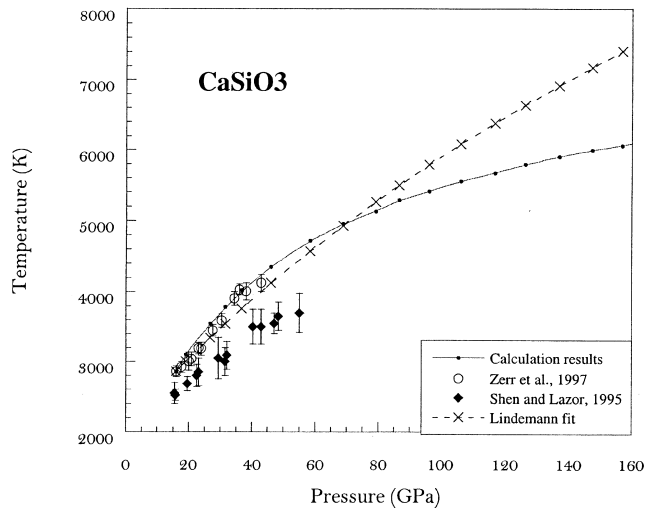


Fig. 7. The melting temperatures of  $\text{CaSiO}_3$  perovskite under high pressures.

perovskite. Therefore, it is no surprise to find excellent agreement between our calculated results and the experimental data of Zerr et al. [31].

Also the estimates by Lindemann melting equation are given in Fig. 7. Even though the duplicated melting curve is located in the existing melting data, it almost shows a straight line. At lower pressures, it can give the melting trend, but at high pressures, the higher slope ( $dT_m/dP$ ) is not compatible with the high pressure behaviors of solids, such as compressibility, becoming a constant at extreme condition. Therefore, the melting curve given by our model predicts well the high pressure behaviors.

### 3.3. $\text{MgSiO}_3$ perovskite

As discovered in recent in-situ X-ray measurements,  $\text{MgSiO}_3$  perovskite ( $Pbnm$ ) can be synthesized at pressures above 23 GPa using a glass or a low pressure phase having the same composition as the starting material [14]. The input parameters are calculated on the basis of the data of Funamori et al. [14]. All parameters involved in the calculation are shown in Table 1. The calculated results of the melting of  $\text{MgSiO}_3$  perovskite are shown in Fig. 8, along with the recent experimental data [3,4,33].

As for  $\text{CaSiO}_3$  perovskite, our calculated results are in good agreement with the experimental data [3,4,33]. Lindemann law cannot provide a satisfactory prediction of the melting temperature of  $\text{MgSiO}_3$  perovskite under high pressures using an orthorhombic ( $Pbnm$ ) structure [5,34], but a cubic structure for  $\text{MgSiO}_3$  perovskite surprisingly gives reasonable results in agreement with the experimental data at the investigated pressure range below 70 GPa [34]. Because Lindemann law only depends on the compressibility ratio of solids ( $V/V_0$ ) and the Gruneison parameter ( $\gamma$ ), the option of an exact phase occurring at the melting boundary becomes very important. Even the

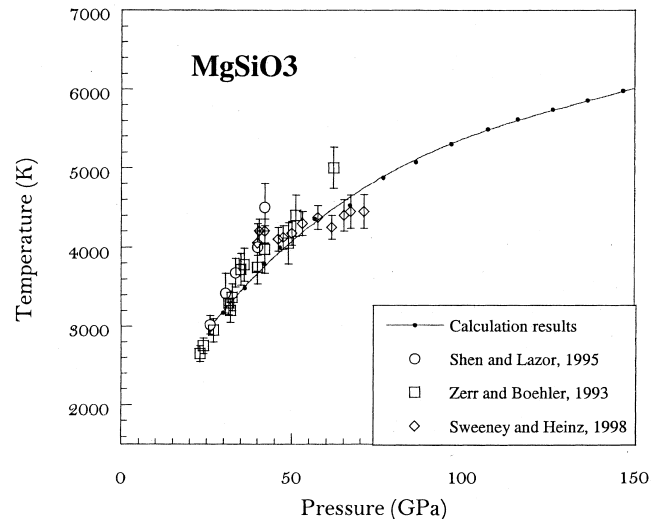


Fig. 8. The melting temperatures of  $\text{MgSiO}_3$  perovskite under high pressures.

results obtained by the Lindemann equation agree with the existing experimental data, it has the same characteristic at high pressure, showing a higher slope ( $dT_m/dP$ ) [34]. For our model, six thermal parameters are used to estimate the melting of  $\text{MgSiO}_3$  perovskite. The effects from temperature and compressibility have been taken into account in our calculation. This weakens the influence of structural factors on the calculations of melting temperatures due to the phase transformations from orthorhombic to cubic lattice structure in  $\text{MgSiO}_3$  induced by temperature. This temperature-induced phase transformation also significantly depends on the thermal expansion of the 8-coordination site occupied by Mg ion due to heating, and thus it may lead to a quite weak effect on the thermodynamic parameters of both phases of  $\text{MgSiO}_3$  perovskite. The estimated results have closely reproduced the melting of  $\text{MgSiO}_3$  perovskite, and also have better predicted the general high-pressure behaviors of solids.

## 4. Conclusion

It has been well demonstrated that our previous model can closely reproduce the melting of stable solids at high pressure by comparison between obtained results and existing experimental data of pyrope [3,21–23]. The improved model is also validated by excellent agreement of our calculated melting temperatures and recent experimental data for  $\text{CaSiO}_3$  and  $\text{MgSiO}_3$  perovskites [3,4,29,33]. It can be assumed to be a reliable model in calculating the melting temperatures of high-pressure phases at high pressures. Compared to the estimates by using the empirical melting equation, it is clear that, to extrapolate the melting temperatures of any solids, our model is more precise and reliable at higher pressures than the empirical melting equation.

## Acknowledgements

We thank the Florida International University for financial support, which made this study possible. Special thanks are due to Debby Arnold whose critical reading greatly improved our manuscript.

## References

- [1] Z. Wang, H. Mao, S.K. Saxena, *J. Alloys Comp.* 299 (2000) 287–291.
- [2] R.E. Cohen, Z. Gong, *Phys. Rev. B* 50 (1994) 12301–12311.
- [3] G. Shen, P. Lazor, *J. Geophys. Res.* 100 (1995) 17699–17713.
- [4] A. Zerr, R. Boehler, *Science* 262 (1993) 553–557.
- [5] J.P. Poirier, *Phys. Earth Planet. Int.* 54 (1989) 364–369.
- [6] Z.W. Wang, *Phys. Earth Planet. Int.* 115 (1999) 219–228.
- [7] A. Karlsson, P. Lazor, *J. Alloys Comp.* 305 (2000) 209.
- [8] F.A. Lindemann, *Phys. Z.* 11 (1910) 609.
- [9] J.J. Gilvarry, *Phys. Rev.* 102 (1956) 308.
- [10] G.C. Kraut, G.C. Kennedy, *Phys. Rev.* 151 (1966) 669.
- [11] Z. Wang, P. Lazor, S.K. Saxena, *Physica B*, in press.
- [12] M. Born, K. Huang, *Dynamical Theory of Crystal Lattices*, Oxford University Press, 1954.
- [13] L.G. Liu, A.E. Ringwood, *Earth Planet. Sci. Lett.* 28 (1975) 209–211.
- [14] N. Funamori, T. Yagi, W. Utsumi, T. Kondo, T. Uchida, M. Funamori, *J. Geophys. Res.* 101 (1996) 8257–8269.
- [15] Y. Wang, D.J. Weidner, F. Guyot, *J. Geophys. Res.* 101 (1996) 661–672.
- [16] O.L. Anderson, in: *Equations of State for Geophysical and Ceramic Sciences*, Oxford University Press, 1995, p. 405.
- [17] O.L. Anderson, D. Isaak, *Rev. Geophys.* 30 (1992) 57–90.
- [18] Z. Wang, F. Tutti, S.K. Saxena, *High T–High P.* 31 (1999) 681–685.
- [19] J. Shanker, S.S. Kushwah, P. Kumar, *Physica B* 223 (1997) 78–83.
- [20] J. Shanker, S.S. Jushwah, *Physica B* 245 (1998) 190–194.
- [21] T. Irifune, E. Ohtani, *J. Geophys. Res.* 91 (1986) 9357–9366.
- [22] J. Zhang, C. Herzberg, *Am. Miner.* 79 (1994) 497–503.
- [23] D.W. Williams, G.C. Kennedy, *J. Geophys. Res.* 74 (1969) 4359–4366.
- [24] L.G. Liu, *Earth Planet. Sci. Lett.* 36 (1977) 237–245.
- [25] M. Kanzaki, *Phys. Earth Planet. Int.* 49 (1987) 168–175.
- [26] T. Irifune, T. Koizumi, J. Ando, *Phys. Earth Planet. Int.* 15 (1996) 90–106.
- [27] S.E. Kesson, J.D. Fitz, J.M.G. Shelly, R.L. Withers, *Earth Planet. Sci. Lett.* 134 (1995) 187–200.
- [28] I. Ahmed-Zaid, M. Madon, *Earth Planet. Sci. Lett.* 129 (1995) 233–247.
- [29] G. Serghiou, A. Zerr, L. Chudinovskikh, R. Boehler, *Geophys. Res. Lett.* 22 (1995) 441–444.
- [30] H.K. Mao, L.C. Chen, R.J. Hemley, A.P. Jephcoat, Y. Wu, *J. Geophys. Res.* 94 (1989) 17889–17894.
- [31] A. Zerr, G. Serghiou, R. Boehler, *Geophys. Res. Lett.* 24 (1997) 909–912.
- [32] T. Yagi, B. O'Neill, T. Kondo, N. Miyajima, K. Fujino, *Eur. J. Miner.* 9 (1997) 301–310.
- [33] J.S. Sweeney, D.L. Heinz, in: M.H. Manghnani, T. Yagi (Eds.), *High Pressure–Temperature Research: Properties of Earth and Planetary Materials*, AGU, 1998, pp. 185–196.
- [34] Z. Wang, S.Y. O'Reilly, W.L. Griffin, H. Zheng, H. Mao, *J. Phys. Chem. Solids* 61 (2000) 1815–1820.